Dalton Transactions

PAPER

View Article Online
View Journal | View Issue

Cite this: *Dalton Trans.*, 2016, **45**, 284

Silver complexation by metallacryptates†

Kevin Lamberts,[a] Matteo Tegoni,*[b] Xiang Jiang,[c] Hui-Zhong Kou*[c] and Ulli Englert*[a]

Received 25th September 2015,
Accepted 12th November 2015

DOI: 10.1039/c5dt03749b

www.rsc.org/dalton

We report the first complete characterization of metallacryptates encapsulating Ag(I) cations: carboxylato ligands derived from L-proline and L-alanine chelate and bridge six Cu(II) centres arranged in a slightly distorted octahedral fashion. Eight oxygen atoms of these ligands are disposed in square-prismatic geometry and coordinate the monovalent cation. Two alternative metallacryptates based on alanine have been identified which differ with respect to aggregation: a solid in which pairs of encapsulating sites are formed competes with an infinite chain of M(I) coordinating sites. In contrast, the individual encrypting moieties are arranged as overall neutral and isolated molecular species in the proline-based metallacryptate. This proline derivative can accomodate Ag(I) and Na(I) cations and form a solid solution. Susceptibility measurements confirm ferromagnetic interactions between the Cu(II) within the hexanuclear proline cryptate and thus underline the similarity between solids accommodating Na(I) and Ag(I). Spectroscopic results suggest that these metallacryptates hardly dissociate in methanol solution.

1. Introduction

Organic crown ethers have proven useful since their discovery in the 1960s.[1] These usually selective ligands are applied as cytotoxic agents,[2] as building units for supramolecular polymers,[3] as templates for crystal engineering[4] and as stabilizers for selective catalysis.[5] J. M. Lehn expanded the realm of polydentate ligands into the third dimension:[6,7] cryptands literally "bury" cations, thus providing even higher stability constants and more pronounced selectivity than 2D crown ethers. Such functionalities are not restricted to organic molecules but may also be exerted by coordination complexes. These so-called metallacrowns[8–12] and metallacryptands[13–15] represent less popular but highly versatile chemical answers to the requirements of polydentate ligands. They may not only coordinate cations but also encapsulate anions;[16,17] sulfate selectivity has been shown for a dinuclear Cu derivative.[18] Quite obviously, the metal-containing polydentate ligands may feature certain extra properties in comparison to their classical organic counterparts, such as metal-based redox activity and the structural manifold of coordination centers with a potentially elevated number of binding sites. Rare earth cations were trapped in a trigonal prismatic hexanuclear Cu(II) scaffold and their magnetic interactions were studied by Sopasis *et al.*[19]

A class of octahedral hexanuclear metallacryptates from Cu(II) perchlorate and L-amino acids shows the capability of binding Na(I) in its cavities: an octahedral arrangement of copper cations, connected by chelating and bridging amino acids, is stabilized by crosslinking perchlorates and the incorporated host cation. Hu *et al.*[20] first reported the synthesis of $Na[Na \subset Cu_2\{Cu(Gly)_2\}_4(ClO_4)_6(H_2O)_2]\cdot 2H_2O$ and $[Na \subset Cu_2\{Cu(Pro)_2\}_4(ClO_4)_4(OH)]\cdot H_2O$. Later, Wang *et al.*[21] published an isomorphous proline metallacryptate and a hydroxyproline metallacryptate and reported their magnetic properties. Further occurrences of this structural motif were encountered for L-alanine,[22] L-threonine[23] and 1-amino-1-cyclopropane.[24] The prototypic organic cryptand [2.2.2] with a cavity size radius of 1.4 Å may coordinate a number of different cations[25] with a preference for K^+. Expanding from a 6 fold coordinating cavity to 8, Xiang *et al.*[23] found that the hexanuclear L-threonine cryptate coordinated Na^+ exclusively, even in the presence of other cations.

In this contribution, we report the first complete structural characterizations of such hexanuclear copper(II)-metallacryptates which incorporate silver cations (see Fig. 1 for their general architecture): $[Ag \subset Cu_2\{Cu(Pro)_2\}_4(ClO_4)_5]$ (**1a**) is closely related to the structural outcome of a competition experiment, the solid solution $[M \subset Cu_2\{Cu(Pro)_2\}_4(ClO_4)_5]$, M = Ag, Na(I) (**1b**). Our investigation does not only cover the structural aspects of these compounds but also extends to their magnetic properties and their stability in solution. We compare these mono-cryptands to two alanine derivatives

[a]*Institute of Inorganic Chemistry, RWTH Aachen, Landoltweg 1, 52074 Aachen, Germany. E-mail: ullrich.englert@ac.rwth-aachen.de; Fax: +49 241 8888288; Tel: +49 241 8094666*

[b]*Department of Chemistry, University of Parma, Parco Area delle Scienze 17A, 43124 Parma, Italy*

[c]*Department of Chemistry, Tsinghua University, Beijing 100084, P. R. China*

†Electronic supplementary information (ESI) available: Further crystallographic refinement details, ESI mass spectra, UV-Vis spectra and dilution titration spectra. CCDC 1048757, 1048758, 1427077 and 1427078. For ESI and crystallographic data in CIF or other electronic format see DOI: 10.1039/C5DT03749B

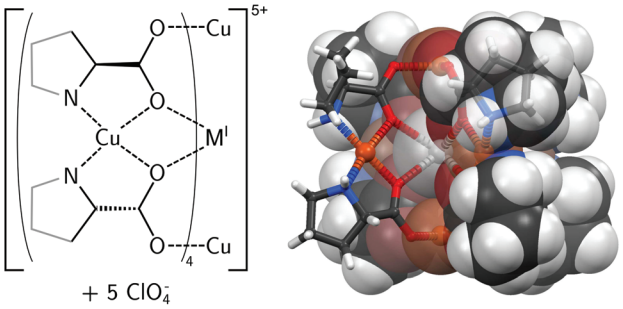

1a: proline, M = Ag
1b: proline, M = Ag/Na-mixture
2a: alanine, M = Ag, dimer
2b: alanine, M = Ag, polymer

Fig. 1 General architecture (left) of the presented metallacryptates and 3-dimensional model of the cation in **1a**.

(**2a** & **2b**) in which dimers or polymers of coordination sites aggregate *via* longer Cu···O Jahn–Teller contacts. As for monovalent Ag(I), no metallacryptates have been described to date, but a flexible metallacrown surrounding this cation has been reported;[26] no structural characterization for this complex has been provided.

2. Experimental

Chemicals were used as purchased without further purification: L-alanine (99.8%, Evonik), L-proline (>99%, Evonik), $CuClO_4{\cdot}6H_2O$ (98%, Sigma-Aldrich), $AgClO_4$ (97%, Sigma-Aldrich), $NaClO_4{\cdot}H_2O$ (99%, Merck), urea (99.5%, Grüssing).

2.1. Synthesis

The metallacryptates have been synthesised by self assembly *via* diffusion of an antisolvent into a stoichiometric solution of the constituents of the target products. X-ray powder diffraction (Fig. 2) confirms phase purity of **1a** and **1b**. The experimental powder patterns were obtained on flat samples at room temperature whereas the simulations are based on single crystal data collected at 100 K. Most solids exhibit positive thermal expansion and therefore larger lattice parameters at higher temperature, corresponding to a shift towards smaller diffraction angles in the experimentally observed patterns. A quantitative determination of the Na content in **1b** is not possible by X-ray powder diffraction, since the diffractogram hardly differs from that of the isomorphous compound **1a**. However, the reflection width indicates a homogeneous distribution of Na and Ag within the bulk sample. The powder diffractogram of the sample containing **2a** and **2b** shows the concomitant presence of both products (visible in the range up to 10° 2θ) together with impurities of L-alanine and at least one unidentified major byproduct.

2.1.1 Synthesis of Cu_2(L-Pro)$_4(H_2O)_3$. Cu_2(L-Pro)$_4(H_2O)_3$ was synthesised similar to literature:[27] $CuSO_4{\cdot}5H_2O$ (10 mmol, 2.496 g, 1 eq.) was dissolved in 10 mL H_2O and L-proline (20 mmol, 2.303 g, 2 eq.) as well as NaOH (20 mmol, 0.8 g, 2 eq.) was added to the solution. Addition of 70 mL of acetone yielded a blue precipitate after 10 minutes of vigorous stirring. Since sodium sulfate precipitated as well, the solid was filtered off and suspended in 200 mL EtOH. Sodium sulfate remained as a solid and was removed by filtration. The filtrate was evaporated with a rotary evaporator and the resulting blue oil solved in 10 mL of H_2O. Addition of 70 mL of acetone yielded blue crystalline powder of $[Cu_2$(L-Pro)$_4(H_2O)_3]{\cdot}2H_2O$. Drying in a dessicator yields Cu_2(L-Pro)$_4(H_2O)_3$ according to microanalysis. Anal. Calcd for Cu_2(L-Pro)$_4(H_2O)_3$: C: 36.6%, H: 5.8%, N: 8.6%, Found: C: 36.8%, H: 5.8%, N: 8.4%.

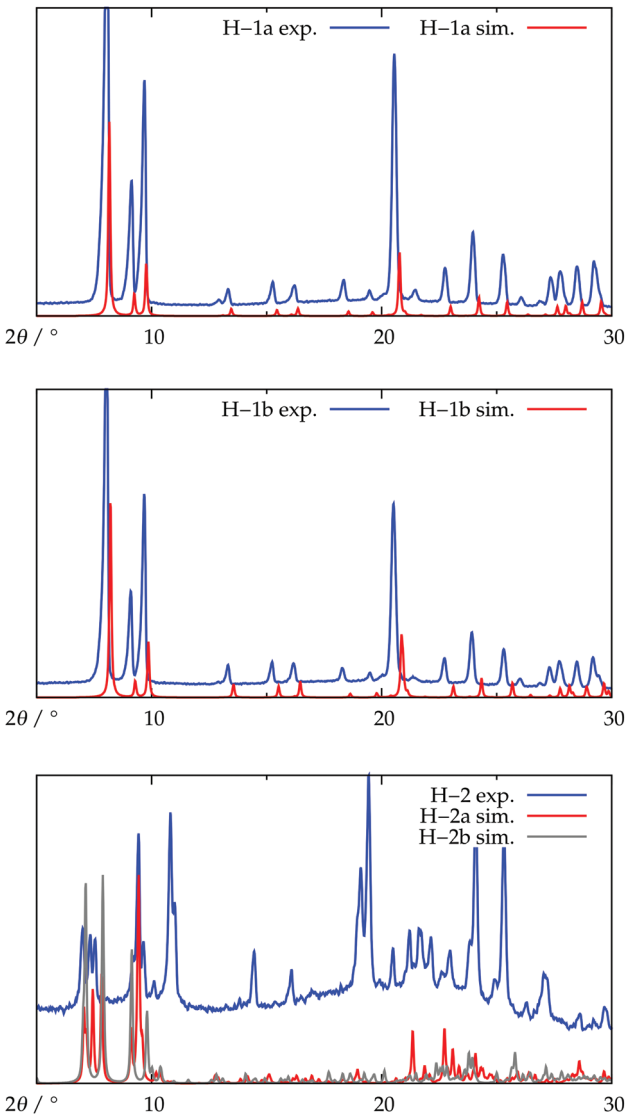

Fig. 2 Experimental (blue) and simulated (red) X-ray powder diffractograms.

2.1.2. Synthesis of 1a. While **1a** can be synthesised in a one step reaction, larger quantities of **1a** could be obtained by dissolving $(Cu_2$(L-Pro)$_4(H_2O)_3)_{0.5}$ (2 mmol, 674 mg, 4 eq.), $CuClO_4{\cdot}6H_2O$ (1 mmol, 371 mg, 2 eq.) and $AgClO_4$ (0.5 mmol, 112 mg, 1 eq.) in 50 mL MeOH and precipitating the product

by adding 100 mL Et_2O. The solid was recovered by filtration and dried in a desiccator.

Anal. Calcd. for **1a**: C: 26.0%, H: 3.7%, N: 6.0%, Found: C: 24.8%, H: 3.8%, N: 5.5%. Single crystals could be grown from a smaller scale reaction in the same stoichiometry, followed by gas phase diffusion of Et_2O into the solution. Crystals grew after 1–2 days as large square bipyramids. The crystals of **1a** are a solvate with the formula $[Ag \subset Cu_2\{Cu(L\text{-}Pro)_2\}_4(ClO_4)_5]\cdot(MeOH)_{0.58}(H_2O)_{0.84}$. The same product was obtained by replacing the $Cu_2(L\text{-}Pro)_4(H_2O)_3$ building block by $CuClO_4\cdot 6H_2O$ and L-proline and performing the reaction with stoichiometric amounts of urea.

2.1.3. Synthesis of 1b. Mixed crystals containing Ag and Na were obtained by dissolving $(Cu_2(L\text{-}Pro)_4(H_2O)_3)_{0.5}$ (2 mmol, 674 mg, 4 eq.), $CuClO_4\cdot 6H_2O$ (1 mmol, 371 mg, 2 eq.), $AgClO_4$ (0.25 mmol, 56 mg, 0.5 eq.) and $NaClO_4\cdot H_2O$ (0.25 mmol, 31 mg, 0.5 eq.) in 50 mL MeOH and precipitating the product by adding 100 mL Et_2O. The solid was recovered by filtration and dried in a desiccator. Single crystals could be grown from a smaller scale reaction in the same stoichiometry, followed by gas phase diffusion of Et_2O into the solution. Crystals grew after 1 day as large square bipyramids and are a solvate with the formula $[Ag_{0.56}Na_{0.44} \subset Cu_2\{Cu(L\text{-}Pro)_2\}_4(ClO_4)_5]\cdot H_2O$.

2.1.4. Synthesis of 2a & 2b. $CuClO_4\cdot 6H_2O$ (3 mmol, 1.1 mg, 6 eq.), L-alanine (4 mmol, 356 mg, 8 eq.) and $AgClO_4$ (0.5 mmol, 112 mg, 1 eq.) were dissolved in 50 mL MeOH and heated under reflux with urea (4 mmol, 270 mg, 8 eq.) for 1 hour. The solvent was removed with a rotary evaporator and a blue oil formed. A small amount of the oil was dissolved in 1 mL MeOH, and Et_2O was allowed to diffuse into the solution *via* the gas phase. After 3 days, blue hexagonal blocks of **2a** and a small number of very long needles of **2b** concomitantly formed from the solution. The crystals are solvates with the formula $[Ag \subset Cu_2\{Cu(L\text{-}Ala)_2\}_4(ClO_4)_5]\cdot(MeOH)_{4.5}$ for **2a** and $[Ag \subset Cu_2\{Cu(L\text{-}Ala)_2\}_4(ClO_4)_5]\cdot(MeOH)_{3.5}(H_2O)_{1.5}$ for **2b**.

2.2. Solid state analysis

Single crystal diffraction experiments were performed on a Bruker D8 goniometer with APEX CCD detector. An Incoatec microsource with Mo-Kα radiation (λ = 0.71073 Å) was used and temperature control was achieved with an Oxford Cryostream 700. Crystals were mounted with grease on glass fibers and data were collected at 100 K in ω-scan mode. Data were integrated with *SAINT-Plus*[28] and corrected for absorption by multi-scan methods with SADABS.[28]

Structures were solved by the Patterson method as implemented in SHELXS[29] and refined by full matrix least squares procedures on F^2 with SHELXL-13.[29] Well ordered non-hydrogen atoms were refined with anisotropic displacement parameters whenever physically reasonable. Hydrogen atoms connected to carbon were placed in idealised positions and included as riding with $U_{iso}(H) = 1.2U_{eq}(C)$ for CH or CH_2 and $U_{iso}(H) = 1.5U_{eq}(C)$ for methyl groups. H atoms attached to amino groups and solvent molecules were either located from difference Fourier maps or placed in idealized positions in order to achieve reasonable hydrogen bond patterns and refined with $U_{iso}(H)$ constrained to multiples of the U_{eq} of the parent atoms. Distance and rigid bond[30] restraints were applied to allow a more stable refinement. The absolute structure parameters were calculated according to Parsons and Flack[31] and confirmed the known chirality of the amino acids (Table 1).

Structure **1b** surprisingly showed a different disorder from that encountered in **1a**. Difference Fourier maps suggested an end-to-end disorder for the axially coordinated moieties, one anion and a solvent molecule. Under these conditions, the additional water/methanol disorder for the latter could not be handled as simply as in the case of **1a**. Only the coordinated oxygen atom was therefore refined with full site occupancy, and the many alternative sites with low fractional site occupancy for methanol C and H atoms were not taken into account.

X-ray powder diffraction was performed at the Institute of Inorganic Chemistry, RWTH Aachen using a Stoe Stadi P diffractometer with Guinier-geometry (Cu-Kα_1, λ = 1.54059 Å, Johannson germanium monochromator and Stoe Imageplate detector IP-PSD, 0.005° stepwidth in 2θ).

Microanalysis was performed at the Institute of Organic Chemistry, RWTH Aachen with a CHN-O-Rapid VarioEL from Heraeus.

3.3. Solution studies

The samples were prepared using reagent-grade methanol or doubly-distilled water. Dilution titration experiments were carried out as follows. Mother solutions of **1**(Na) (*ca.* 5.4 mM) or **1a** (*ca.* 5.0 mM) were prepared by weight in methanol or water. Proper volumes of the solutions were diluted 1 : 1 to obtain samples diluted of a factor of 2. Successive dilutions allowed to obtain samples with dilution factors of 4, 8, 16, 32, 64, and 128. Analogous samples of **1**(Na) were prepared by diluting the methanolic or aqueous mother solution of the compound with a 0.1 M $NaClO_4$ solution in methanol or water, respectively. The most diluted solutions of these sample set had concentrations in the 32.6–40.2 μM range. Visible spectra of samples of $Cu_2(L\text{-}Pro)_4(H_2O)_3$ (*ca.* 6 mM) and $Cu(ClO_4)_2\cdot 6H_2O$ (*ca.* 50 mM) prepared by weight in methanol were used to calculate the molar absorbance of the compounds in this solvent. Visible spectra of the samples were collected in the 400–900 nm interval using a Thermo Evolution Bio 260 UV-visible spectrophotometer provided with a Peltier device. Quartz cuvettes of 0.1, 1 and 5 cm path length were used.

ESI mass spectra were recorded using a WatersAcquity SQ Detector with ESI interface and a direct infusion device. Data were processed by using the spectrometer software (MassLinx 4.1). The measurements were performed on solutions of **1**(Na) or **1a** in methanol, water, or methanol : water mixtures 9 : 1 (v : v). The sample concentration was *ca.* 10^{-4} M. Direct infusion analyses were always performed at 10 μL min^{-1}. Experimental conditions were as follows: ES capillary 3.0 kV; cone 30–80 V; extractor 4 V; source block temperature 80 °C; desolvation temperature 150 °C; cone and desolvation gas (N_2)

Table 1 Crystallographic details of the structures [M ⊂ Cu_2{Cu(amino-carboxylate)$_2$}$_4$(ClO_4)$_5$]·solvent

Compound/CCDC#	**1a**/1048757	**1b**/1048758	**2a**/1427077	**2b**/1427078
Crystal data				
Chemical formula	$C_{40.58}H_{68}N_8AgCl_5Cu_6O_{37.42}$	$C_{40}H_{66}N_8Ag_{0.56}Cl_5Cu_6Na_{0.44}O_{37}$	$C_{57}H_{132}N_{16}Ag_2Cl_{10}Cu_{12}O_{81}$	$C_{55}H_{130}N_{16}Ag_2Cl_{10}Cu_{12}N_{16}O_{82}$
M(I), amino-carboxylate	Ag(I), L-Pro	$Ag(I)_{0.56}Na(I)_{0.44}$, L-Pro	Ag(I), L-Ala	Ag(I), L-Ala
Solvent	0.58 MeOH 0.84 H_2O	H_2O	4.5 MeOH	3.5 MeOH 1.5 H_2O
M_r	1933.07	1880.44	3670.50	3660.46
Crystal system, space group	Tetragonal, *I*4	Tetragonal, *I*4	Triclinic, *P*1	Monoclinic, $P2_1$
a (Å)	13.512(3)	13.4554(16)	12.7360(7)	9.8711(12)
b (Å)			12.8490(8)	24.766(3)
c (Å)	18.097(6)	17.931(2)	19.6150(12)	5.596(3)
α (°)			104.7400(10)	
β (°)			97.6700(10)	100.770(2)
γ (°)			95.1970(10)	
V (Å^3)	3304.2(18)	3246.4(9)	3050.4(3)	6147.2(13)
Z	2	2	1	2
μ (mm^{-1})	2.49	2.41	2.70	2.67
Crystal size (mm)	0.24 × 0.23 × 0.09	0.14 × 0.09 × 0.07	0.16 × 0.14 × 0.08	0.22 × 0.14 × 0.04
Data collection				
T_{min}, T_{max}	0.533, 0.745	0.609, 0.745	0.648, 0.746	0.581, 0.746
No. of measured, independent and observed [$I > 2\sigma(I)$] reflections	18924, 3532, 2912	19001, 3116, 2651	47383, 34212, 27196	93433, 35809, 22713
($\sin\theta/\lambda_{max}$) (Å^{-1})	0.634	0.611	0.714	0.718
R_{int}	0.083	0.068	0.030	0.080
Refinement				
$R[F^2 > 2\sigma(F^2)]$, w$R(F^2)$, *S*	0.054, 0.150, 1.04	0.042, 0.115, 1.04	0.055, 0.135, 1.03	0.080, 0.188, 1.01
No. of reflections	3532	3116	34 212	35 809
No. of parameters	241	241	1516	1504
No. of restraints	159	149	260	320
$\Delta\rho_{max}$, $\Delta\rho_{min}$ (e Å^{-3})	0.93, −0.89	1.20, −0.42	3.02, −3.12	1.67, −1.92
Flack parameter	0.04(2)	−0.019(14)	0.017(9)	0.074(7)

1.6 and 8 L min^{-1}, respectively. Scanning was performed at *m*/*z* 100–2000.

The distribution diagrams of the complex species for the Cu^{2+}/proline system was studied with the Hyss 2006 program.[32]

3. Results and discussion

Four new metallacryptates are presented. They share a very similar architecture with respect to primary cation coordination: four *cis*-bis-L-aminocarboxylato-copper(II) units are connected *via* their *exo*-carboxylato-O atoms towards two copper(II) cations.

An octahedral arrangement of 6 copper cations is formed, leaving a coordination pocket in the middle that offers an eightfold binding site by the *endo*-carboxylato-O atoms. This site is occupied by Ag(I) (or statistically occupied by Ag(I) and Na(I) in the case of the solid solution **1b**). Four perchlorate anions bridge the equatorial Cu-units so that an overall monocationic metallacryptate motif is formed.

The metallacryptates **1a–2b** differ with respect to the arrangement of the primary cation coordination sites. Structures **1a** and **1b** are synthesised from L-proline. **1a** is isomorphous to its Na-analogue[21] (here referred to as **1**(Na)) and very closely related to the solid solution of a mixture of both (**1b**). Since these compounds are monomeric structures (axial copper cations are coordinated by solvent or the remaining perchlorate anion, see Fig. 3) **1a** was suited for investigations on its magnetic properties and solution behaviour. Moreover, studies on the stability of **1**(Na) and **1a** in aqueous and methanolic solutions were carried out.

Structures **2a** and **2b**, synthesised from L-alanine, remarkably are not isomorphous to their related Na compounds.[22] Both exhibit the aforementioned general architecture. **2a** however, is a dimer of two connected metallacryptate units, **2b** is a polymer with two crystallographically independent strands.

Structural key points and distinctive features will be discussed for all compounds. The magnetic properties and solution behaviour of **1a** will be presented separately.

3.1. Structural properties of 1a and 1b

The metallacryptate in **1a** consists of four neutral *cis*-bis-L-prolinato-copper(II) units. They connect the two axial Cu(II)-cations and the central Ag(I), thus resulting in a formally pentacationic aggregate. The charge is compensated by one terminal and four bridging ClO_4^- anions. Disordered solvent MeOH and H_2O are incorporated in the solid.

1a forms as a phase pure solid in almost quantitative yield by self assembly of its constituents in the stoichiometry required for the formation of the target product: **1a** can be obtained by evaporation of methanolic solution of the reactants $Cu(ClO_4)_2$, L-proline and $AgClO_4$ in a 6 : 8 : 1 ratio.

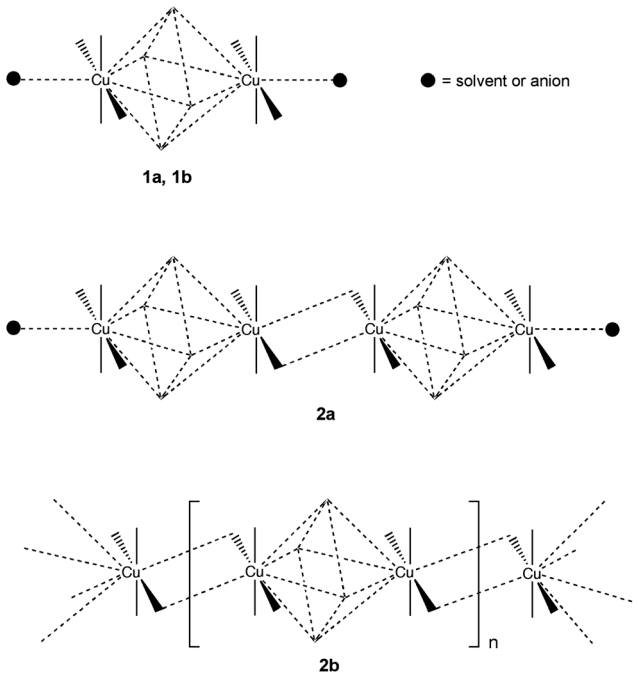

Fig. 3 Schematic representation of the supramolecular connectivity of the octahedral metallacryptate units (black dots representing solvent or anions).

A stepwise approach as reported elsewhere for the Na-analogue[21] is not necessary. However, addition of 8 equivalents urea and its decomposition at elevated temperature benefits the crystallisation, while the sodium analogue already precipitates as powder under those conditions. Crystals of **1a** are blue and up to 2 mm large; their tetragonal bipyramidal morphology matches the crystal class of the solid. The metallacryptate **1a** is derived from enantiopure L-proline and therefore must crystallize in a chiral space group, in the present case space group *I*4 (no. 79). The heteronuclear cation exhibits exact fourfold and approximate local D_4 symmetry (Fig. 4), with the central Ag(I) and both axial Cu(II) cations on the crystallographic axis (Wyckoff position 2*a*).

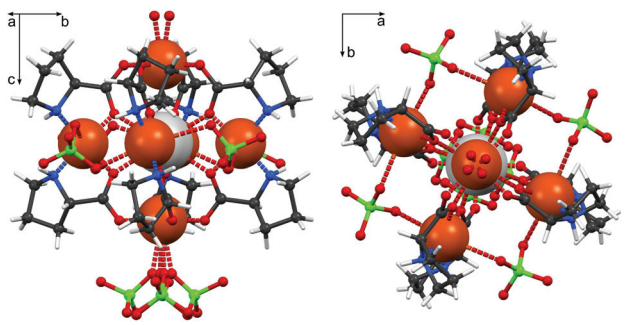

Fig. 4 Molecule of **1a** indicating octahedral metal arrangement. Color code: Ag – grey, Cl – green, Cu – orange, C – black, H – white, N – blue, O – red.

The encrypted metal is coordinated by one oxygen atom of each proline and thus enclosed in a slightly distorted square prismatic coordination sphere, with a torsion angle between the top and bottom square planes of the oxygen prism of *ca.* 10°. The six Cu(II) cations, two associated with the base planes and four with the lateral edges of the prism, adopt a slightly clinched octahedral geometry ($Cu\cdots Cu_{axial}$ = 6.960(10) Å, $Cu\cdots Cu_{equatorial}$ = 7.131(3) Å) about the central Ag(I). A more detailed inspection of the coordinative bonds in the cation reveals that axial and equatorial Cu(II) differ: the former are in a typical Jahn–Teller type square pyramidal coordination, with short Cu–O bonds (*ca.* 2 Å) to the amino acid ligands and significantly longer contacts to either a perchlorate counter anion (*ca.* 2.5 Å) or a coordinated solvent molecule (*ca.* 2.3 Å). The cations in the equatorial *cis*-bis-L-prolinato-copper(II) units are O,N chelated by short bonds to the amino acid molecules. In addition to this square planar coordination, they interact with much more distant (2.7–2.9 Å) bridging perchlorate anions. Selected bond distances for all structures are given in Table 3. Precise geometry data and their standard uncertainties have been compiled in the ESI.† The pentacationic complex and the bridging or terminal perchlorate anions aggregate *via* the above-mentioned longer Cu···O distances, and hence **1a** can, despite its formal composition as a salt, be described as a solid built from discrete "molecules". Fig. 4 shows two projections of a $[Ag \subset Cu_2\{Cu(Pro)_2\}_4(ClO_4)_5]$ aggregate in the [100] and [001] view directions.

A view along [100] also illustrates the arrangement of the aggregates in the body-centered unit cell (Fig. 5). The axial residues are disordered about the crystallographic fourfold axis and fill the cavities **A** (terminal perchlorate) and **B** (methanol/water solvent molecule).

The framework around the silver cation can be seen as [2.2.2.2] metallacryptate. The diagonal length of the square prismatic cage amounts to *ca.* 5.1 Å; when a certain degree of flexibility is taken into account, the coordination cage may enclose a range of cations. Selectivity of cryptands does, however, not only depend on radii criteria but also on additional parameters such as Pearson hardness[33] or the bite angle of the ligands. The cation selectivity in metallacryptates has been addressed by Wang *et al.*[21] These authors shortly mention the selectivity of heir L-proline cryptate towards Na(I) in presence of Li(I) or K(I) and add that an analogous reaction with Ag(I) is possible. Additionally, they comment on a possible existence of metallacryptates in solution. However, no sophisticated evidence is given.

For the case of our $Cu_2\{Cu(L\text{-}Pro)_2\}_4(ClO_4)_5$ metallacryptate, we have obtained structural evidence for the inclusion of both silver and sodium cations under competitive conditions. When the templated assembly of the cryptate is conducted as above but from an equimolar mixture of $AgClO_4$ and $NaClO_4$, a solid solution is obtained in which both monovalent cations are incorporated in roughly 1 : 1 ratio. This solid **1b** has also been structurally characterized. The most relevant result concerns selectivity: The significantly different electron density of both alternative M(I) cations allows to refine their occupancy with good accuracy. **1b** contains 56.3(6)% Ag *versus* 43.7(6)% Na,

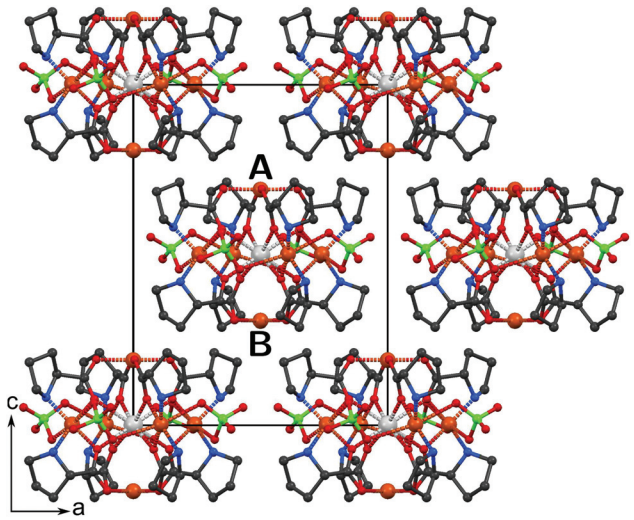

Fig. 5 View of the body-centered unit cell of **1a**. The terminal ligands fill the voids A and B; they are disordered about the fourfold axes and have been omitted.

indicating a slight preference for silver coordination. In X-ray powder diffraction, reflections of **1b** are of similar width as those of **1a**, thus indicating a homogenous solid solution.

The most prominent effects of partial Na substitution are observed in the geometry of the coordination cage and changes in the geometry of the Cu octahedron. For eightfold coordination the crystal radius of Na(I) is 0.1 Å shorter than that of Ag(I).[34] As a consequence, the M(I)–O distances shorten (M–O = 2.553(6) and 2.544(7) Å) and the overall geometry of the cryptate adopts a more symmetric arrangement: the differences in length between the edges within the Cu_6 octahedron are reduced by an order of magnitude. Table 2 summarizes the structural differences between **1a**, **1b** and the Na(I) analogue[21] (measured at room temperature).

Table 2 Geometric differences of **1a**, **1b** and the Na(I) analogue **1**(Na)[22] (measured at room temperature) and the two polymorphs from alanine **2a** and **2b**

	1a	**1b**	**1**(Na)
σ_{oct} (Cu_6) [grd^2]	0.262	0.057	0.029
$\Delta_{oct} \times 10^3$ (Cu_6)	0.155	0.047	0.017
Cu1···Cu3 [Å]	6.960	6.972	7.011
Cu2···Cu2^{i} [Å]	7.131	7.031	7.058
	2a		**2b**
σ_{oct} (Cu_6) [grd^2]	14.172, 13.270		5.232, 3.701
$\Delta_{oct} \times 10^3$ (Cu_6)	0.026, 0.062		0.138, 0.091
Cu2···Cu3 [Å]	7.114(2)		7.024(3)
Cu4···Cu5 [Å]	7.130(2)		7.052(3)
Cu1_1···Cu1_3 [Å]	7.112(2)		7.180(9)
Cu1_2···Cu1_4 [Å]	7.095(2)		7.207(6)
Cu1_5···Cu1_7 [Å]	7.146(2)		7.189(5)
Cu1_6···Cu1_8 [Å]	7.107(2)		7.127(9)

$\sigma_{oct} = \frac{1}{11}\sum_{i=1}^{12}(\theta_i - 90°)^2$; $\Delta_{oct} = \frac{1}{6}\sum_{i=1}^{6}[(l_i - \bar{l})/\bar{l}]^2$; l_i: shortest M(I)···Cu; θ_i: smallest Cu···M(I)···Cu; $^{i}1 - x, 1 - y, z$.

Table 3 Selected bond distances of Structures **1a**, **1b**, **2a**, and **2b**

Distance	**1a** [Å]	Distance	**1b** [Å]
Ag1–O1	2.585(10)	Ag1–O1	2.553(6)
Ag1–O3	2.553(10)	Ag1–O3	2.544(7)
Cu1–O9	2.45(2)	Cu1–O9A	2.380(17)
Cu2–O5	2.709(12)	Cu2–O5	2.703(7)
Cu2–O6^{i}	2.879(15)	Cu2–O6^{i}	2.738(8)
Cu3–O13	2.223(19)	Cu3–O9B	2.30(2)
Distance	**2a** [Å]	Distance	**2b** [Å]
Ag1–O1_1	2.593(7)	Ag1–O1_1	2.570(13)
Ag1–O1_2	2.451(7)	Ag1–O1_2	2.583(11)
Ag1–O1_3	2.635(7)	Ag1–O1_3	2.672(12)
Ag1–O1_4	2.650(6)	Ag1–O1_4	2.654(12)
Ag1–O3_1	2.618(7)	Ag1–O3_1	2.665(12)
Ag1–O3_2	2.771(6)	Ag1–O3_2	2.651(11)
Ag1–O3_3	2.568(6)	Ag1–O3_3	2.579(13)
Ag1–O3_4	2.548(7)	Ag1–O3_4	2.568(11)
Cu1_1–O5_1	2.782(8)	Cu1_1–O5_1	2.585(15)
Cu1_1–O6_2	2.535(8)	Cu1_1–O6_4	2.504(17)
Cu1_2–O5_2	2.621(8)	Cu1_2–O5_2	3.136(17)
Cu1_2–O6_3	2.554(8)	Cu1_2–O6_1	2.484(18)
Cu1_3–O5_3	2.541(7)	Cu1_3–O5_2	2.710(16)
Cu1_3–O5A_4	2.931(6)	Cu1_3–O5_3	2.431(10)
Cu1_4–O5_1	2.606(7)	Cu1_4–O5_4	2.513(16)
Cu1_4–O5A_4	2.707(7)	Cu1_4–O6_3	2.569(15)
Cu2–O1	2.216(8)	Cu2–O4_1^{ii}	2.478(9)
Cu3–O4_5	2.372(6)	Cu3–O2_3^{iii}	2.457(10)
Ag2–O1_5	2.476(7)	Ag2–O1_5	2.686(10)
Ag2–O1_6	2.528(8)	Ag2–O1_6	2.573(13)
Ag2–O1_7	2.602(7)	Ag2–O1_7	2.600(11)
Ag2–O1_8	2.731(7)	Ag2–O1_8	2.664(13)
Ag2–O3_5	2.769(7)	Ag2–O3_5	2.577(11)
Ag2–O3_6	2.694(7)	Ag2–O3_6	2.617(12)
Ag2–O3_7	2.635(7)	Ag2–O3_7	2.709(11)
Ag2–O3_8	2.489(7)	Ag2–O3_8	2.536(13)
Cu1_5–O5_5	2.644(8)	Cu1_5–O5_5	3.07(2)
Cu1_5–O6_6	2.577(8)	Cu1_5–O5_8	2.592(14)
Cu1_6–O5_8	2.938(8)	Cu1_6–O5_5	2.581(17)
Cu1_6–O6_5	2.548(8)	Cu1_6–O5_6	2.633(13)
Cu1_7–O6A_7	2.561(6)	Cu1_7–O5_7	2.639(16)
Cu1_7–O5_8	2.601(8)	Cu1_7–O6_6	2.520(16)
Cu1_8–O5_6	2.551(8)	Cu1_8–O5_8	3.209(13)
Cu1_8–O5A_7	2.503(7)	Cu1_8–O6_7	2.486(13)
Cu4–O2	2.243(6)	Cu4–O4_7^{iii}	2.409(10)
Cu5–O4_2	2.409(6)	Cu5–O2_5^{ii}	2.463(10)

Symmetry code: $^{i}y, 1 - x, z$; $^{ii}-1 + x, y, z$; $^{iii}1 + x, y, z$.

Diffraction data of crystalline **1b**, despite its substitutional disorder for the encrypted M(I) cation, are of higher quality than those for the pure Ag(I) compound **1a**. A tentative explanation for this at first sight unexpected behaviour can be that the significantly more regular constituents in **1b** are compatible with a more efficient packing.

3.2. Magnetic properties of 1a

The presence of magnetically active Cu(II) cations within the metallacryptates suggests that susceptibility measurements can contribute additional information to a comparison between closely related Na(I) and Ag(I) coordinating species. The former information has been provided by Wang *et al.*[21]

and later summarised for other Na(I) containing cryptates by Xiang *et al.*[23]

Temperature-dependent magnetic susceptibility measurement for **1a** was carried out on a Quantum Design SQUID magnetometer. The experimental susceptibility was corrected for the diamagnetism of the constituent atoms (Pascal's Tables). Temperature-dependent magnetic susceptibilities of **1a** were measured in the temperature range of 2–300 K under an applied magnetic field of 2000 Oe.

As shown in Fig. 6, the $\chi_m T$ value at 300 K is 2.5 $cm^3\ mol^{-1}$ K, which is slightly larger than the theoretical value of 2.25 $cm^3\ mol^{-1}$ K for six spin-only Cu(II) ions (S = 1/2, g = 2). Furthermore, the $\chi_m T$ value increases upon temperature cooling, indicating the presence of overall ferromagnetic interaction between adjacent Cu(II) centers. The χ_m^{-1} *versus* T data above 25 K were fitted by the Curie–Weiss law, giving a Curie constant of 2.52 $cm^3\ mol^{-1}$ K and a Weiss constant of 1.55 K, which also evidences the presence of ferromagnetic interaction within the Cu_6. In this octahedral Cu_6 cluster, the magnetic coupling between the equatorial Cu(II) atoms and axial Cu(II) atoms *via* the *syn–anti* carboxylate groups dominates and can be reasonably considered as identical. The magnetic coupling between the equatorial Cu(II) atoms *via* the central diamagnetic Ag^+ pathway is negligible. Thus, the exchange coupling constant J is evaluated to be +0.77(1) cm^{-1} with a g value of 2.12(1) by using the equation reported before.[23] The positive J value further confirms the ferromagnetic interaction within Cu_6 cluster.

For each Cu(II) ion with a distorted square pyramidal or elongated octahedral configuration, the unpaired electrons occupy the magnetic orbital $d_{x^2-y^2}$. For a *syn–anti* bridging mode of carboxylate, the 2p orbitals of two oxygen atoms respectively linked to the two Cu(II) ions are oriented to unfavourably give a strong orbital overlap for antiferromagnetic coupling. Therefore, most *syn–anti* carboxylate-bridged Cu(II) complexes display ferromagnetic interaction.[23,35–44]

For complex **1a**, the adjacent $d_{x^2-y^2}$ orbitals from equatorial and axial position of the octahedral Cu_6 cluster are nearly perpendicular to each other with the dihedral angle between the N_2O_2 and O_4 coordination planes of 75.86°. According to the strict orthogonality of the magnetic orbitals of Cu(II) ions, such perpendicular arrangement of magnetic orbitals of adjacent Cu(II) atoms would lead to the overall ferromagnetic interaction.[37] Moreover, the nonplanarity of the Cu–O–C–O–Cu linkages further weakens the orbital overlap to invalidate the antiferromagnetic interaction,[41] which contributes to the overall ferromagnetic coupling in complex **1a**. DFT calculation results also corroborate the ferromagnetic nature of Cu(II)–Cu(II) magnetic coupling *via* the *syn–anti* carboxylate bridge.[44]

3.3. Results of solution studies of 1a, 1b and 1(Na)

In contrast to organic cryptands, the metallacryptates are formed by self assembly of linkers and labile coordination centers; the question arises to which extend this process will be reversible. Do the complex architectures exist in solution or rather undergo disassembly to generate the Cu-prolinate and Cu(II) ions?

We decided to get insights on the integrity in solution of the metallacryptates containing Na^+ (**1**(Na)) and Ag^+ (**1a**). We therefore started with collecting the ESI-MS spectra of compounds **1**(Na) and **1a** in methanol ($c_{\mathbf{1}(Na),\mathbf{1a}}$ *ca.* 100 μM) by direct infusion of the solution. Signals corresponding to copper complexes were observed in positive-ion mode. In the 1000–2000 m/z range the spectrum of **1**(Na) presents only one significant multiplet at m/z = 1715 (base peak) consistent with the metallacryptate species $\{NaCu_2[Cu(Pro)_2]_4(ClO_4)_4\}^+$ ([Na ⊂ $Cu_2[Cu(Pro)_2]_4(ClO_4)_4$] (Fig. 7 and S4†). Surprisingly, the same peak was observed also in the spectrum of **1a** together with peaks at m/z = 1037, 1315 (base peak) and 1733 (Fig. 8 and S4†).

These latter three peaks, less intense, are present also in the spectrum of **1**(Na). Possibly more surprisingly, none of the

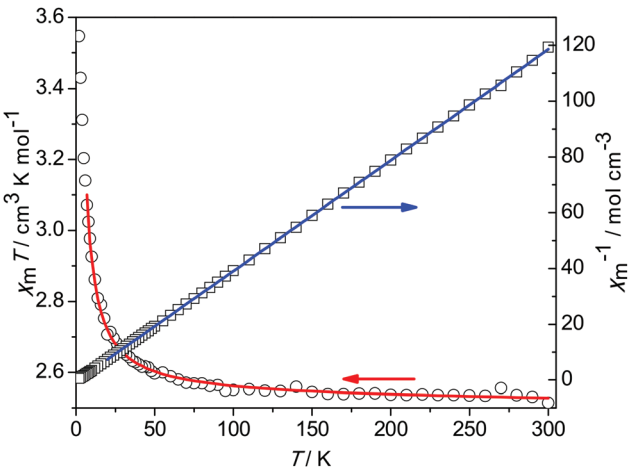

Fig. 6 $\chi_m T$ and χ_m^{-1} *versus* T plots for complex **1a**. The solid lines represent fitting results using the parameters listed in the text.

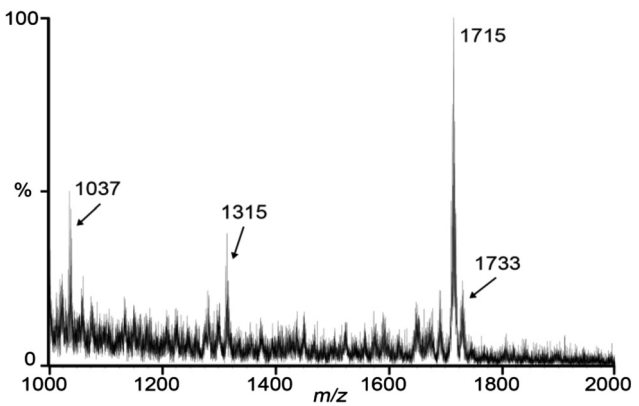

Fig. 7 Positive-ion ESI mass spectrum of a 100 μM solution of **1**(Na) in methanol.

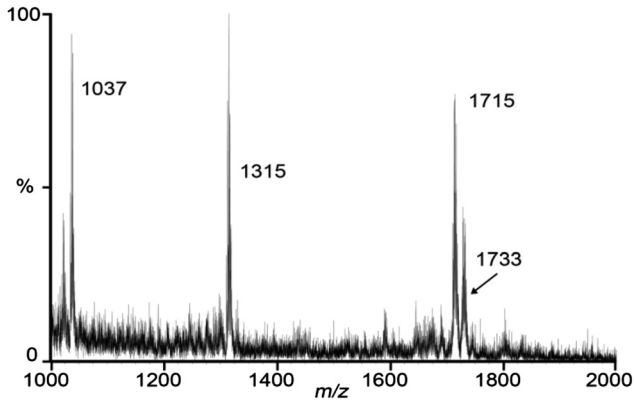

Fig. 8 Positive-ion ESI mass spectrum of a 100 μM solution of **1a** in methanol.

peak in the spectrum of **1a** is associated to Ag^+ species, but rather to the aquated Na^+ metallacryptate (m/z = 1733, $NaCu_2[Cu(Pro)_2]_4(ClO_4)_4(H_2O)$) or to a fragment of the metallacryptate construct (m/z = 1037, $Cu(II)[Cu(Pro)_2]_3(ClO_4)^+$). The base peak at m/z = 1315 has been interpreted as a fragment of the metallacryptate interacting with one sodium and one potassium ion ($\{NaKCu[Cu(Pro)_2]_3(ClO_4)_3(H_2O)\}^+$, the latter being possibly an impurity in the solution. These results show that the metallacryptate scaffold does not result into a complete disaggregation in pure methanolic solution, although they also suggest that the Ag-containing compound **1a** is less stable than its sodium analogue **1**(Na) under ionization conditions. Importantly, no signals above m/z = 1000 were observed for solutions of **1**(Na) or **1a** in water (Fig. S5†), while spectra similar to those obtained in pure methanol were observed for samples prepared in methanol/water 9 : 1 (v/v) mixtures (Fig. S6 and S7†). These data confirm the metallacryptates are completely disaggregated in aqueous samples, likely as the result of favourable solvation effects of the components of the construct. However, our data suggest that the compounds do not undergo a complete dissociation when water in methanol amounts to up to 10% in volume.

If we consider Cu^{2+} and $[Cu(Pro)_2]$ as fragments (components) of the metallacryptate scaffold, then we can describe the assembly process of **1**(Na) and **1a** through the equilibrium $Na^+(Ag^+) + 2Cu^{2+} + 4[Cu(Pro)_2] + 4ClO_4^- = \{Na(Ag)Cu[Cu(Pro)_2]_4(ClO_4)_4\}^+$. The related stoichiometric equilibrium constant $K = [\text{metallacryptate}]/([Na^+]\,[Cu^{2+}]^2[\{Cu(Pro)_2\}]^2[ClO_4^-]^4)$ has the dimension of a M^{-8}. Therefore this equilibrium is concentration dependent, and favoured at higher concentrations.

Among these components, $[Cu(Pro)_2]$ and Cu^{2+} (as $Cu(ClO_4)_2$) have a λ_{max} of absorption in the visible range of 606 and 829 nm in methanol, respectively (λ_{max} = 619 and 810 nm in water, Fig. S8 and S9†). The molar absorption of $[Cu(Pro)_2]$ is significantly higher than that of the Cu^{2+} ion in both methanol (ε_{max} = 68 and 11 M^{-1} cm^{-1}, respectively) and in water (ε_{max} = 51 and 12 M^{-1} cm^{-1}, respectively). On the other hand, the metallacryptates **1**(Na) and **1a** absorb at λ_{max} *ca.* 660 nm in methanol, respectively (ε = *ca.* 350 M^{-1} cm^{-1}, Fig. S8†), while in water their absorption is at slightly lower wavelengths (λ_{max} = 651 and 652 nm, respectively, ε = *ca.* 250 M^{-1} cm^{-1}, Fig. S9†). In both solvents, the absorption maxima of **1**(Na) and **1a** are intermediate between those of $[Cu(Pro)_2]$ and Cu^{2+}.

With these data in our hands, we decided to study the disaggregation processes of the metallacryptates in solution through dilution experiments monitored by visible absorption spectrophotometry. In the hypothesis that disaggregation of the metallacryptate construct occurs upon dilution, then a blue shift from λ_{max} *ca.* 655 toward 610 nm should be observed, as the consequence of the appearance of $[Cu(Pro)_2]$ which is largely more absorbing than Cu^{2+}. On the contrary, if the metallacryptates are already fully dissociated even in the most concentrated solution, then the λ_{max} should not vary significantly upon dilution.

Indeed, by dilution of solutions of both **1**(Na) and **1a** (*ca.* 5 mM to 33–40 μM; 128-fold dilution), we observed a significant 18–19 nm blue shift of the λ_{max} (Fig. 9 and S10†). On the contrary, when the same experiments were performed in water the λ_{max} remained constant up to 8-fold dilution, moving toward higher wavelengths (red shift) at lower concentrations (Fig. 10 and S11†).

The blue shift observed in methanol, and not observed for aqueous solutions, indicates that a progressive dissociation of **1**(Na) and **1a** is obtained in this medium upon dilution. This result is consistent with ESI MS data which suggested the presence of undissociated metallacryptate at 10^{-4} M concentration. On the other hand, the red shift observed for higher dilutions in water could be very well interpreted taking into account the dissociation of $[Cu(Pro)_2]$ which occurs at lower concentrations following the $[Cu(Pro)_2] = [Cu(Pro)]^+ + Pro^-$ equilibrium. Because the formation constants of copper(II) and proline complexes in water are known[45–47] we could quantitatively calculate the concentration of the species at the equilibrium. The speciation of the system is reported in Fig. 11A and it refers to a Cu^{2+}/proline = 6 : 8 corresponding to a fully dissociated metallacryptate in unbuffered solution. In this system the most

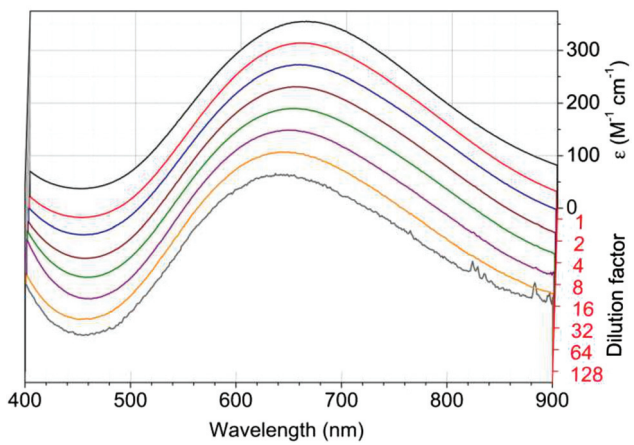

Fig. 9 Spectra of the dilution titration of **1**(Na) in methanol (5.01 mM diluted to 39.2 μM, no background salt added).

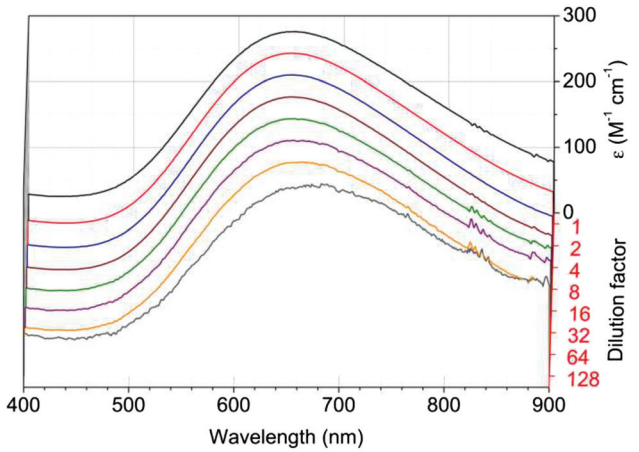

Fig. 10 Spectra of the dilution titration of **1**(Na) in water (5.14 mM diluted to 40.2 μM, no background salt added).

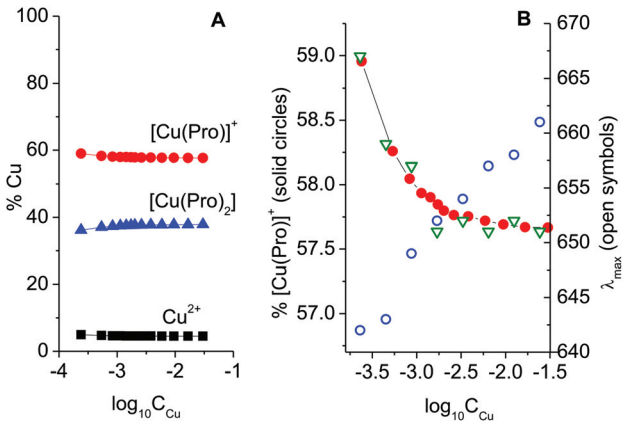

Fig. 11 A: Speciation diagram of the Cu^{2+}/proline system (Cu : Pro = 6 : 8, C_{Cu} = 30 mM, unbuffered solution). B: Red circles: plot of the % $[Cu(Pro)]^+$ in the system Cu : Pro = 6 : 8 at different total Cu^{2+} concentrations (red circles). Green triangles: experimental λ_{max} values for the dilution of a solution of **1**(Na) in water, and in methanol (blue circles).

abundant species is the $[Cu(Pro)]^+$ complex (*ca.* 58%). As $[Cu(Pro)_2]$ absorbs at 610 nm while $[Cu(Pro)]^+$ at *ca.* 710 nm,[48] the mixture of the two species should result into an intermediate λ_{max}, consistent with the observed 655 nm in water. The concentration of $[Cu(Pro)_2]$ remains constant up 8-fold dilution, and then it starts to decrease with a concomitant increase of the amount of $[Cu(Pro)]^+$. This results into the red shift, as represented in Fig. 11B: the trend in shift as higher wavelenghts overlaps very well with the increase in concentration of $[Cu(Pro)]^+$.

Very interestingly, similar experiments were carried out also on **1**(Na) diluted with either 0.1 M methanolic or aqueous $NaClO_4$ solution (Fig. S12 and S13,† experiments using **1a** resulted into precipitation issues). The results are similar to those obtained with pure solvents, but the presence of sodium perchlorate in methanol the blue shift amounts to only 11 nm. Although from this experiments we cannot discriminate the effect of the sodium and perchlorate ions separately, the results suggest that the presence of a high concentration of these ions prevents, as expected, the dissociation of the metallacryptate. On the contrary, the high concentration of sodium perchlorate has no effects in aqueous solutions where the metallacryptate **1**(Na) remains fully dissociated.

Overall, our results suggest that the dissociation of **1**(Na) and **1a** is complete in water regardless of the total metallacryptate concentration and the presence of perchlorate ions in the medium. On the contrary, in methanol the dissociation occurs at a minor extent. The absence of polymetallic species in aqueous solutions is fully consistent with the speciation of the Cu^{2+}/amino acid (L) systems in aqueous solution: where the side chain of the amino acid is non-coordinating, $[Cu(L)_2]$ and $[Cu(L)]^+$ are the major species with no reported formation of polynuclear complexes.[45–47] Moreover, our results explain how polymetallic species containing amino acids can be conveniently crystallized from methanolic solutions. Finally, as the behaviour of **1**(Na) and **1a** in the dilution experiments is not significantly different, we should conclude that the stability of the two proline metallacryptates is not very different.

3.4. Structural properties of 2a and 2b

The coordinating amino acid (L-proline in the case of **1a** and **1b**) plays an important role for the formation of metallacryptates. Ag(I) coordination can also be achieved with L-alanine; in this case, the concomitant products **2a** and **2b** have been obtained. With respect to primary cation coordination, they closely correspond to the proline derivatives: four *cis*-bis-alaninato-copper(II) connect two axial Cu(II)-cations and enclose an Ag(I) in their centre. However, the alanine-based cryptates are considerably more distorted from an ideal fourfold symmetry, and additional coordinative bonds link primary metallacryptate sites to overall more complex solids.

2a crystallises in *P*1 as a dimer. The two cryptate molecules are connected *via* two Cu–O contacts of axial copper atoms (Cu–O *ca.* 2.39 Å). The alternative product **2b** on the other hand crystallises in $P2_1$ with a slightly longer connection between metallacryptate subunits (Cu–O *ca.* 2.45 Å). However, the two symmetry independent molecules are linked on both sides towards its neighbour and hence build two independent polymer chains extending along *b* (Fig. 12).

While the connection of the metallacryptate molecules to more extended aggregates is the most distinctive difference between the products from proline and alanine, the local symmetry of the hexanuclear units of **2a** and **2b** is also significantly different. With all atoms on general positions the C_4 (or approximate D_4) symmetry is broken. This is reflected in the coordination environment around the silver cation: Ag–O distances range from *ca.* 2.45 to 2.77 Å in **2a** and 2.54 to 2.71 Å in **2b**. The base planes of the distorted square prismatic coordination polyhedron are almost not tilted towards each other although this geometry is hard to parametrise since all Ag–O distances are independent. The overall octahedral arrangement of the copper cations is also much more variable (see

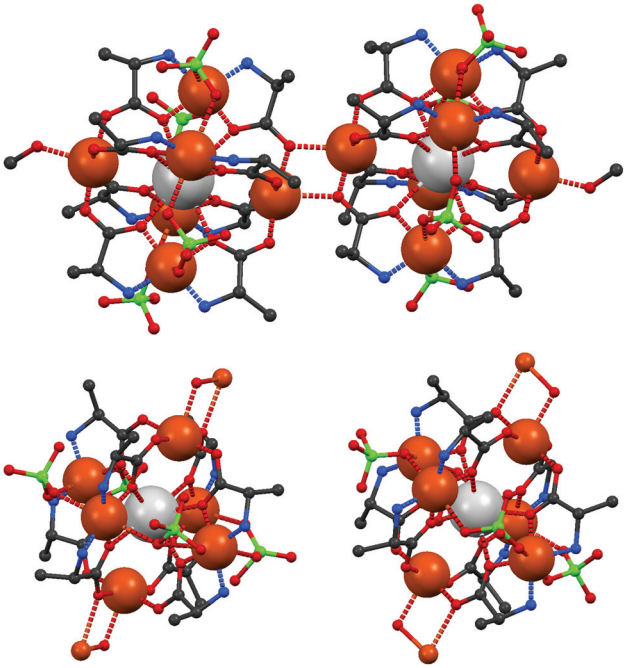

Fig. 12 Dimeric structure of **2a** (top) and chain segments of the double polymer strands of **2b**.

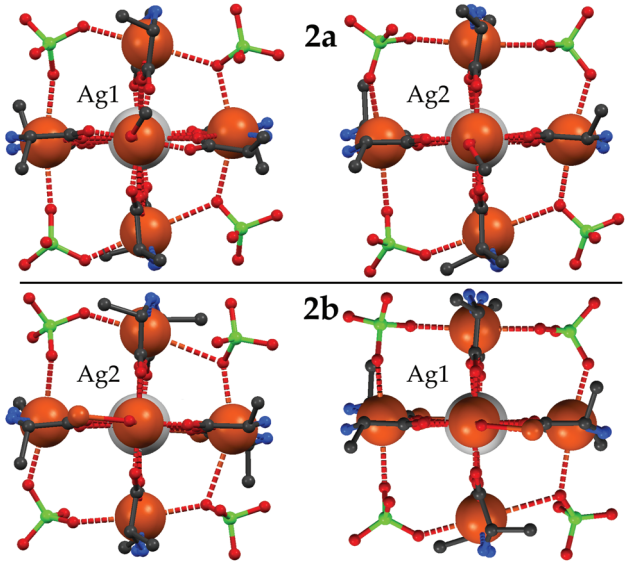

Fig. 13 Bridging of the *cis*-bis-alaninato-copper(II) units by perchlorate anions in structures **2a** and **2b**.

Table 2). While Cu···Ag···Cu angles have a much broader distribution than in the metallacryptates from proline, their Cu···Ag distance distribution is comparable. Distances across the octahedron are around 7.1 Å in **2a**. In **2b** they are shorter in chain direction (7.04 Å) than perpendicular to the chain (7.18 Å). Cu···Cu distances along the edges range from 4.657(2) to 5.338(2) Å in **2a** and from 4.89(1) to 5.30(1) Å in **2b**.

Most notably, the bridging of the *cis*-bis-alaninato-copper units with perchlorate anions shows a larger variety: in both structures O–Cl–O bridging similar to that in **1a** or **1b** can be observed. Additionally, direct bridging with only one oxygen atom of the perchlorate anion occurs. Each compound features one symmetrically independent metallacryptate site in which only one pair of neighbouring Cu(II) centers is directly bridged (Fig. 13, right) and a second residue in which two of these Cu–O–Cu connections occur (Fig. 13, left).

While we showed that for the case of proline both cations, Na(I) and Ag(I), yield isomorphous or closely related molecular solids, the structures from alanine show polymorphism in the case of both cations and all structures are actually quite different: three structures are known for the analogue Na(I) chemistry.[22] While one of the structures is not a metallacryptate with a full shell as presented here, the other two polymorphs are a molecular structure similar to **1a** and **1b**, and a dimeric structure comparable to **2a** but with additional $NaClO_4$ bridging. To our knowledge **2b** is therefore the first axially connected polymer of hexanuclear metallacryptates of its kind. However, a polymeric connection has been reported for a metallacryptate from hydroxyproline,[21] though its connection is *via* the peripheral hydroxy groups.

4. Conclusions

What can be learned from Ag(I) coordination by metallacryptates, and perhaps more general, how do metallacryptates compare to their organic counterparts?

The proline-based metallacryptands **1a** and **1b** suggest that Na(I) and Ag(I) complexation will not lead to very different results: both cations may form a solid solution with the same metallacryptand, and the pure Ag(I) and Na(I) species are closely related solids with similar magnetic properties and similar stabilities in solution. One might be tempted to consider these results for the proline derivatives as predictable, but the corresponding alanine compounds convey a very different message. Ag(I) complexation by alanine-based metallacryptates is entirely different from Na(I) complexation. Three different Na(I) cryptates form based on the applied stoichiometry. One adopts a structure analogous to **1a**; the second arranges in a dimeric fashion like **2a** but contains additional $NaClO_4$ connecting the molecules. The third structure is a partial metallacryptate that is connected to an infinite polymer chain. Here, one bis-alaninato-copper unit is missing for the full hexanuclear cryptate arrangement.

Metallacryptates and organic cryptands differ in a very obvious aspect: the organic multidentate ligands might adopt alternative conformations when non-coordinating but they will surely not completely dissociate and be present as possible major constituent in solutions of specific solvents such as methanol. The characterization of metallacryptates to date mostly relies on solid state methods, but the results concerning their existence in solution, never reported previously, are encouraging. In our future work we will attempt to further bridge the gap between solid state characterization and

dynamic behaviour in solution and gain an overall better understanding of the versatile class of metallacryptates.

Acknowledgements

The authors thank Evonik Industries for providing the amino acids. Support from DAAD and BMBF in the framework of the Strategic Partnership RWTH Aachen University – Tsinghua University is gratefully acknowledged. The Marie Curie IRSES "METALLACROWNS" project is acknowledged (https://sites.google.com/site/metallacrowns). The research leading to these results has received funding from the European Community's Seventh Framework Programme (FP7/2007–2013) under grant agreement n° 611488.

References

1 C. J. Pedersen, *J. Am. Chem. Soc.*, 1967, **89**, 7017–7036.
2 D. B. Smithrud, X. Wang, P. Tarapore and S.-M. Ho, *ACS Med. Chem. Lett.*, 2013, **4**(27), 31.
3 B. Zheng, F. Wang, S. Dong and F. Huang, *Chem. Soc. Rev.*, 2012, **41**, 1621–1636.
4 C. Fiolka, I. Pantenburg and G. Meyer, *Cryst. Growth Des.*, 2011, **11**, 5159–5165.
5 V. Leich, K. Lamberts, T. P. Spaniol and J. Okuda, *Dalton Trans.*, 2014, **43**, 14315–14321.
6 B. Dietrich, J. M. Lehn and J. P. Sauvage, *Tetrahedron Lett.*, 1969, **34**, 2885–2888.
7 J. M. Lehn, *Acc. Chem. Res.*, 1978, **11**, 49–57.
8 M. S. Lah and V. L. Pecoraro, *Comments Inorg. Chem.*, 1990, **11**, 59–84.
9 F. C. J. M. van Veggel, W. Verboom and D. N. Reinhoudt, *Chem. Rev.*, 1994, **94**, 279–299.
10 Y. Kobuke, K. Kokubo and M. Munakata, *J. Am. Chem. Soc.*, 1995, **117**, 12751–12758.
11 G. Mezei, C. M. Zaleski and V. L. Pecoraro, *Chem. Rev.*, 2007, **107**, 4933–5003.
12 M. Tegoni and M. Remelli, *Coord. Chem. Rev.*, 2012, **256**, 289–315.
13 M. S. Lah, B. R. Gibney, D. L. Tierney, J. E. Penner-Hahn and V. L. Pecoraro, *J. Am. Chem. Soc.*, 1993, **115**, 5857–5858.
14 B. R. Gibney, A. J. Stemmler, S. Pilotek, J. W. Kampf and V. L. Pecoraro, *Inorg. Chem.*, 1993, **32**, 6008–6015.
15 R. W. Saalfrank, A. Dresel, V. Seitz, S. Trummer, F. Hampel, M. Teicher, D. Stalke, C. Stadler, J. Daub, V. Schünemann and A. X. Trautwein, *Chem. – Eur. J.*, 1997, **3**, 2059–2062.
16 Z. Zhang, J.-Q. Lu, D.-F. Wu, Z.-L. Chen, F.-P. Liang and Z.-L. Wang, *CrystEngComm*, 2012, **14**, 1354–1363.
17 S. Banerjee, N. N. Adrash and P. Dastidar, *CrystEngComm*, 2013, **15**, 245–248.
18 N. N. Adrash, D. A. Tocher and P. Dastidar, *New J. Chem.*, 2010, **34**, 2458–2469.
19 G. J. Sopasis, A. B. Canaj, A. Philippidis, M. Siczek, T. Lis, J. R. O'Brien, M. M. Antonakis, S. A. Pergantis and C. J. Milios, *Inorg. Chem.*, 2012, **51**, 5911–5918.
20 S.-M. Hu, W.-X. Du, J.-C. Dai, L.-M. Wu, C.-P. Cui, Z.-Y. Fu and X.-T. Wu, *Dalton Trans.*, 2001, 2963–2964.
21 L.-Y. Wang, S. Igarashi, Y. Yukawa, Y. Hoshino, O. Roubeau, G. Aromí and R. E. P. Winpenny, *Dalton Trans.*, 2003, 2318–2324.
22 S.-M. Hu, S.-C. Xiang, J.-J. Zhang, T.-L. Sheng, R.-B. Fu and X.-T. Wu, *Eur. J. Inorg. Chem.*, 2008, 1141–1146.
23 S.-C. Xiang, S.-M. Hu, J.-J. Zhang, X.-T. Wu and J.-Q. Li, *Eur. J. Inorg. Chem.*, 2005, 2706–2713.
24 W. Ghattas, R. Ricoux, H. Korri-Youssoufi, R. Guillot, E. Rivière and J.-P. Mahy, *Dalton Trans.*, 2014, 7708–7711.
25 J. M. Lehn and J. P. Sauvage, *J. Chem. Soc. D*, 1971, 440–441.
26 S. H. Seda, J. Janczak and J. Lisowski, *Eur. J. Inorg. Chem.*, 2007, 3015–3022.
27 R. P. Sartoris, L. Ortigoza, N. M. C. Casado, R. Calvo, E. E. Castellano and O. E. Piro, *Inorg. Chem.*, 1999, **38**, 3598–3604.
28 Bruker AXS Inc., *SAINT-Plus and SADABS*, Madison, Wisconsin, USA, 2008.
29 G. M. Sheldrick, *Acta Crystallogr., Sect. C: Cryst. Struct. Commun.*, 2015, **71**, 3–8.
30 F. L. Hirshfeld, *Acta Crystallogr., Sect. A: Cryst. Phys., Diffr., Theor. Gen. Cryst.*, 1976, **A32**, 239–244.
31 S. Parsons and H. Flack, *Acta Crystallogr., Sect. A: Fundam. Crystallogr.*, 2004, **60**, s61.
32 L. Alderighi, P. Gans, A. Ienco, D. Peters, A. Sabatini and A. Vacca, *Coord. Chem. Rev.*, 1999, **184**, 311–318.
33 R. G. Pearson, *J. Am. Chem. Soc.*, 1963, **85**, 3533–3599.
34 R. D. Shannon, *Acta Crystallogr., Sect. A: Cryst. Phys., Diffr., Theor. Gen. Cryst.*, 1976, **32**, 751–767.
35 E. Colacio, J.-P. Costes, R. Kivekas, J.-P. Laurent and J. Ruiz, *Inorg. Chem.*, 1990, **29**, 4240–4246.
36 E. Colacio, J.-M. Dominguez-Vera, J.-P. Costes, R. Kivekas, J.-P. Laurent, J. Ruiz and M. Sundberg, *Inorg. Chem.*, 1992, **31**, 774–778.
37 R. Baldoma, M. Monfort, J. Ribas, X. Solans and M. A. Maestro, *Inorg. Chem.*, 2006, **45**, 8144–8155.
38 D. K. Towle, S. K. Hoffmann, W. E. Hatfield, P. Singh and P. Chaudhuri, *Inorg. Chem.*, 1988, **27**, 394–399.
39 P. Cheng, D. Liao, S. Yan, Z. Jiang, G. Wang, X. Yao and H. Wang, *Inorg. Chim. Acta*, 1997, **254**, 371–373.
40 S. K. Dey, B. Bag, K. M. A. Malik, M. S. El Fallah, J. Ribas and S. Mitra, *Inorg. Chem.*, 2003, **42**, 4029–4035.
41 S. Mukhopadhyay, P. B. Chatterjee, D. Mandal, G. Mostafa, A. Caneschi, J. van Slageren, T. J. R. Weakley and M. Chaudhury, *Inorg. Chem.*, 2004, **43**, 3413–3420.
42 D. Valigura, M. Melnik, M. Koman, L. Martiska, M. Korabik, J. Mrozinsky and T. Glowiak, *Polyhedron*, 2004, **23**, 2447–2456.
43 S. Konar, P. S. Mukherjee, M. G. B. Drew, J. Ribas and N. R. Chaudhuri, *Inorg. Chem.*, 2003, **42**, 2545–2552.

44 A. Rodríguez-Fortea, P. Alemany, S. Alvarez and E. Ruiz, *Chem. – Eur. J.*, 2001, **7**, 627–637.
45 I. Sovago, T. Kiss and A. Gergely, *Pure Appl. Chem.*, 1993, **65**, 1029–1080.
46 L. D. Pettit and H. K. Powell, *The IUPAC Stability Constants Database*, Royal Society of Chemistry, London, 1992–2000.
47 R. M. Smith, A. E. Martell and R. J. Motekaitis, *NIST Critically Selected Stability Constants of Metal Complexes, Database 46, 7.0*, Gaithersburg, MD, USA, 2003.
48 E. Prenesti, M. Daniele, M. Prencipe and G. Ostacoli, *Polyhedron*, 1999, **18**, 3233–3241.